The Use of Diffractive Imitator Optics as Calibration Artefacts

Paul C T Rees[*a], John B. Mitchell[a], Andy Volkov[a], Jean-Michel Asfour[b], Frank Weidner[b], Alexander G. Poleshchuk[c], Ruslan K. Nasyrov[c]

[a]Glyndŵr University, National Facility for Ultra-Precision Surfaces, The OpTIC Centre, St Asaph Business Park, Wales LL17 0JD; [b]DIOPTIC GmbH, Bergstraße 92A, D-69469 Weinheim, Germany; [c]Institute of Automation and Electrometry, Siberian Branch of Russian Academy of Sciences, Novosibirsk, 630090, Russian Federation

ABSTRACT

The testing of highly aspheric optics often requires complex test arrangements: these test systems can be multi-element and will have both fabrication and alignment errors present in the test wavefront. It may not be feasible to calibrate such systems with conventional optical shop practice. The use of diffractive imitator optics, with carefully controlled fabrication uncertainties, can be used to characterise these systems.

We describe the use of reflective imitator CGH optics as calibration artefacts in the calibration of an optical test system used to test ELT primary mirror segments. The optical test system is designed to have two operational modes: one to measure a spherical reference optic; and one to measure the primary mirror segment. The use of diffractive imitators in this test system is designed to provide traceability between these two operational configurations, to quantify residual alignment aberrations, and to quantify fabrication errors in the test system. We outline the design of the optical test system, the design of three imitator CGH artefacts required to provide traceability between the two optical test modes, and our calibration approach.

We demonstrate the calibration performance achieved with this approach. Without the use of these imitator artefacts, the absolute accuracy of the optical test is estimated to be 149 nm RMS wavefront, of which 47 nm RMS is attributed to midspatial wavefront errors and 141 nm RMS is attributed to alignment and prescription errors. The repeatability of this calibration has been established as better than 3 nm wavefront standard deviation, with an absolute accuracy of 19 nm RMS wavefront.

Keywords: CGH, diffractive imitator, optical test, interferometry, calibration

1. INTRODUCTION

Practical optical test systems for the testing of off-axis aspheric surfaces are often multi-element and can include optical surfaces which are not symmetric. Because the nulling wavefront for testing aspherical surfaces will not be symmetric, conventional optical shop procedures for quantifying the residual errors in the optical test cannot be applied. In these cases, a reference artefact of some kind must be used. Any conventional reference artefact must itself be fabricated to high accuracy. An alternative is to use a diffractive artefact.

In this paper we describe the use of diffractive artefacts to quantify residual wavefront errors in an existing optical test: a test designed for the fabrication of aspherical ELT primary mirror segments[1]. These diffractive artefacts were designed to imitate part of the optical test system as ideal components, allowing the calibration of the test to high accuracy.

2. TESTING ELT SEGMENTS

ESO E-ELT Prototype M1 segments

During the Phase B of the ESO (European Southern Observatory) E-ELT design programme, ESO let two contracts within Europe, each to manufacture a set of E-ELT prototype primary mirror (M1) segments to its 42 m M1 optical design specification.

*paul.rees@glyndwr.ac.uk; phone 44 1745 535210; fax 44 1745 535101

The nominal M1 prescription for these prototype segments was

$$R_0 = 84000.0 \text{ mm} \tag{1}$$

$$k_0 = -0.993295 \tag{2}$$

For this optical surface, the aspheric departure for each segment increases from the centre to the edge of the primary mirror. The aspheric departure for each segment is dominated by astigmatic form and coma. The peak-valley (PV) of both these terms increases from the centre of M1 to its edge, as does the mean radius of curvature (ROC) of the segment. Figure 1 plots aspheric departure against radial distance from the centre of M1, for a subsurface (i.e. segment) of 1520 mm diameter, tilted such that the normal to the tangent plane at the centre of the segment is aligned to the optical axis of the test. Figure 1 also plots the behavior of principal aspheric forms, expressed as Zernike terms, against radial distance from the centre of M1. The remaining aspheric departure after removal of ROC variation, astigmatism, coma and trefoil has a maximum PV of approximately 0.2 micrometres.

The radial positions of the ESO prototype E-ELT segments are presented in Table 1.
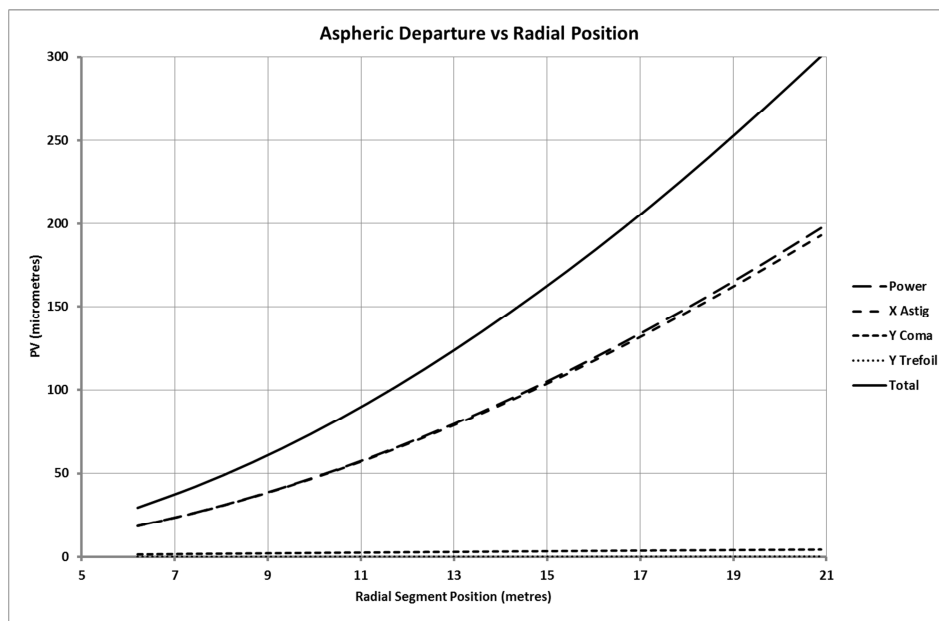

Figure 1. A plot of aspheric departure with radial position of the prototype M1 segments. For consistency, the "Total" departure includes the variation of power with radial position. The trefoil component lies along the bottom of the graph.

Table 1. Radial position of the centre of each identified prototype M1 segment in metres. S3 is the centre of this cluster of segments.

Prototype Segment	Radial Position (m)
S1 (RR15AA15)	18.47
S2 (RR16AA01) and **S4** (RR16AA15)	19.10
S3 (RR16AA16)	19.68
S5 (RR17AA01) and **S7** (RR17AA18)	20.31
S6 (RR17AA17)	20.89

Interferometric Testing of E-ELT Prototype Segments

One challenge for the manufacture of ELT segments is the full-aperture optical test. The primary mirror in the original 42 m E-ELT design is ellipsoidal in form, tessellated so that the mirror is made up of 984 individual segments of non-regular hexagonal shape. The 984 segments have a six-fold symmetry, meaning that there is a total of 164 (=984/6) individual optical prescriptions for manufacturing the whole primary mirror. The optical test itself must accommodate a range of segment mean radii from 84456 mm for the innermost segment to 89199 mm, the outermost segment, and must be configurable to each of the 164 segment prescriptions.

In the Glyndŵr University optical test, the variation in segment mean ROC and the principle segment aspheric departures of astigmatism and coma are removed using refractive optics. The remaining wavefront departure is removed using a small transmission CGH (computer generated hologram).

The advantage of this optical test arrangement is the ability to test all E-ELT primary mirror segments with one test. Figure 2 presents a schematic of the Glyndŵr University optical test, illustrating the optical layout of the test. Based upon a Twyman-Green interferometer, the test is not substantially common path, meaning that its optical path length of approximately 32 m is vulnerable to the wavefront effects of air mixing and their impact upon testing times, and to non-common-path wavefront errors. Figure 3 presents a photograph of the actual test system in use, in-situ above a CNC polishing machine. For the manufacture of a small number of prototype segments this arrangement kept infrastructure costs low, removed the need to provide handling and alignment facilities for both polishing and testing and lowered the risk of handling damage to the optics.

The technical 'cost' of such a complex test system lies in the management of residual aberrations in the optical test. The test has fourteen optical surfaces between the interferometer diverger lens and the test optic. Of these, eight are optically flat, five are aspherical and one is spherical.

Cost and schedule require that all optics need to be manufactured to known acceptable tolerances, even those of high-precision. For this optical test, quantifying mid-spatial wavefront errors was considered particularly important because all refractive optics and one large spherical mirror, used to compress the 84 m ROC beam, were finished using MRF$^{®}$ (magnetorheological finishing) treatment; known to leave a mid-spatial signature on fabricated optical surfaces. Whilst the critical alignment sensitivities can be identified and managed during the design phase of any test system, its integration will be to a set of measurable tolerances that will also result in some residual wavefront error. In service, the residual wavefront error resulting from the fabrication of the optical test must be characterized and removed either experimentally or numerically.

3. CALIBRATION

Calibrating a Complex Optical Test System

Calibration of an optical test system requires the test wavefront and its residual error to be quantified in a way that is traceable to the International standard of length. The rigour with which this is applied in the fabrication of large optics varies with both the technical requirements for the manufactured optic and the practices of the manufacturer. Plano and spherical optics present a calibration challenge for the optical fabrication industry that is well understood. For aspheric surfaces, the route to a traceable calibration becomes increasingly complex as the aspheric departure of the optic, and thereby the test wavefront, increases and as the form goes from circularly symmetric to fully asymmetric. In addition, for large optics and optics of large aspect ratio, opto-mechanical considerations become increasingly important with the size of the surface to be calibrated.

Figure 2. A schematic of the Glyndŵr University E-ELT prototype segment optical test. The top figure is a detail of the optical breadboard on which the refractive optics are integrated. A spider assembly and small fold mirror diverts the beam emanating from the breadboard to the top sphere at the top of the test tower and then to the optic under test on the polishing machine. The top sphere is instrumental in reducing the optical path length of the test from a nominal 160 m to approximately 32 m.
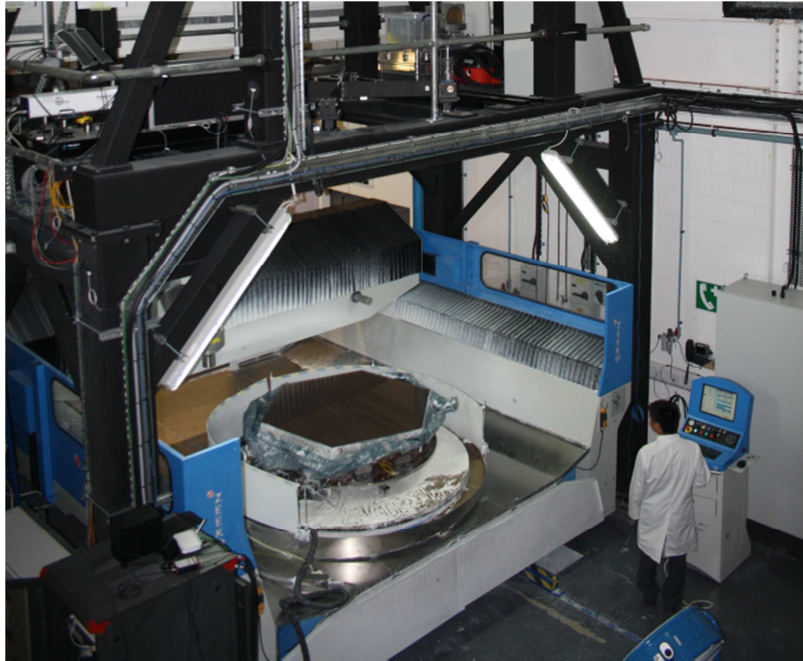
Figure 3. The ELT segment test in use at Glyndŵr University measuring a prototype E-ELT segment.

For optical fabricators the objectives of calibration can vary: absolute determination of ROC; the absolute determination of expected optical aberrations; the absolute determination of mid-spatial wavefront errors; the measurement of the effects of microroughness. In respect of the prototype E-ELT segment test at Glyndŵr University, the calibration objectives are as follows:

1. To establish an absolute ROC calibration for the optical test system

2. To determine the residual low-order wavefront aberrations emanating from the optical test

3. To quantify the mid-spatial wavefront errors emanating from the test system

The absolute ROC of the interferometric test was established using a reference sphere of known ROC of 84165.5 ± 8.2 mm. This reference sphere was also used to quantify the residual low-order aberrations and mid-spatial effects in the test system in one optical configuration. However, to calibrate the optical test system in the configuration used to test the prototype E-ELT segments presented in Table 1, this reference sphere cannot be used because of the magnitude of the aspheric departure. To measure the residual wavefront errors in the test configuration used to measured ELT segments requires traceability to be established between these two test configurations. This is implemented using diffractive imitators.

Calibration Approach

The calibration objective is to quantify the residual wavefront errors in the beam emanating from the optical breadboard (Figure 2) in each of the two operating configurations of the optical test:

1. Configuration to measure a reference sphere of known ROC;

2. Configuration to measure an ELT segment of aspheric form (E-ELT prototype segment).

Configuration (1) is a test configuration to control optical power in the test system, and also to assist in quantifying residual wavefront errors in the optical test. This configuration fully nulls the design wavefront. Configuration (2) is a test configuration to measure an aspheric optic during its fabrication. Because this test configuration is not fully nulled, this design will incorporate a residual wavefront error when correctly aligned.

The diffractive imitators are reflection CGH artefacts manufactured to a high accuracy. Each imitator is designed to imitate the wavefront returned from:

1. Configuration 1 – a perfectly fabricated top sphere (Figure 2) and reference sphere – CGH1

2. Configuration 2 – a perfectly fabricated top sphere and prototype segment number S3 (Table 1) – CGH3

Each imitator is designed to be introduced into the test 120 mm above a small fold mirror, 170 mm beyond an intermediate focus in the test. In this way, the calibration artefacts can be introduced and aligned in the optical system without disturbing the operational configuration of the optical test. In the absence of optical fabrication residuals (including those of the imitator CGHs), prescription drift and breadboard optical misalignments, the imitator test and the non-imitator test should produce identical measured wavefronts in each configuration.

To provide traceability between these two defined configurations, a third imitator is required – CGH2. This imitator is fabricated to have a region that is equivalent to CGH1 in prescription and another that is equivalent in prescription to CGH3. This alignment imitator allows the alignment of CGH1 to be propagated correctly to that of CGH3.

Figure 4 presents a sketch of the imitator CGHs, along with photographs of the fabricated artefacts.
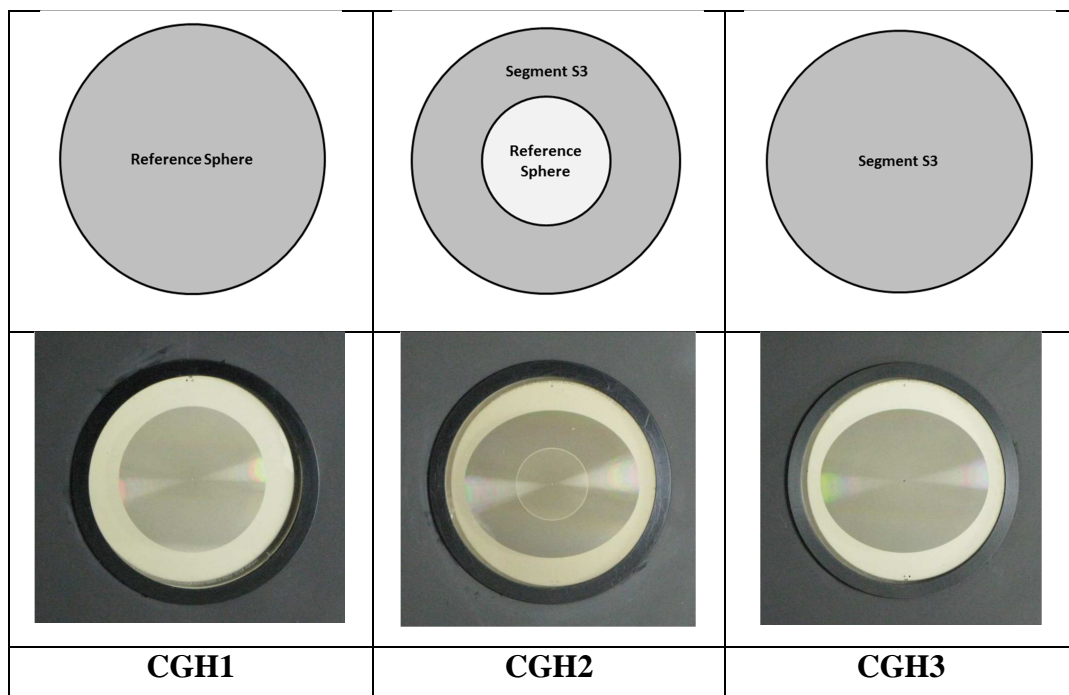

Figure 4. A sketch of each of the diffractive imitator CGHs. Note the elliptical shape of the outer region of CGH2 and of CGH3. Also note the two pattern regions in CGH2. The smallest dimension of the grating region is approximately 44 mm in each CGH.

CGH Fabrication and Accuracy

Each CGH diffractive imitator was designed using the test optical design as a reference. The objective was to design a diffractive imitator that would behave as an ideal optical system beyond the insertion position of the imitator.

The CGH patterns were fabricated using a circular laser writing system CLWS-300IAE[2]. The complex diffractive structure of the imitator CGHs were fabricated by direct laser writing onto chromium films using a resistless technology[3].

The fabrication accuracy of each imitator included provision for following:

1. Residual design error (negligible)

2. Substrate flatness

3. CGH print coordinate errors

4. CGH print rotational accuracy

The writing accuracy of non-rotationally symmetric structure is defined by the resolution of the angular encoder of the CLWS. It has $2.5 \cdot 10^6$ positions per revolution, corresponding to a spacing of 0.1 µm at 25 mm radius. This means the writing error is not significantly higher than for rotationally symmetric patterns and the total error is usually dominated by the substrate flatness.

For CGH1, the expected wavefront error due to these sources was estimated to be 4.0 nm RMS wavefront. For CGH3, this estimated wavefront error was 7.6 nm RMS.

To ensure the relative positioning of the individual CGHs among one another, fiducials were produced outside the CGH on the substrate. Their relative positioning was monitored during the bonding process of the glass substrates into the metal cell. The relative positioning of the three CGHs with respect to each other is better than 20 µm (laterally) and <0.02° (rotationally). The reproducibility of the positioning of the CGHs in the frame is <5 µm (laterally) and <0.004° (rotationally).

Imitator CGH Alignment

Good control of the alignment of each diffractive imitator is critical to accurately quantify the residual wavefront error from the optical test breadboard assembly. For CGH artefacts designed to be aligned within a spherical incident wavefront, it is normal practice to add retro-reflecting alignment features to the CGH that can be monitored via the interferometer. In this case, the incident wavefront on both the CGH1 and CGH3 was highly aberrated. This made the provision of alignment artefacts difficult. Instead, the symmetric shape of the wavefront incident upon CGH1 was used to centre CGH1 to the incident beam. This centration was then propagated to CGH 3 via the two patterns printed on CGH2.

Table 2 presents the aberration sensitivities to residual misalignments for CGH1, derived from the optical design of the test calibration. It can be seen from Table 2 that the critical alignments are the tilt of the imitator about the X- and Y-axes, both of which rapidly incur coma in the observed wavefront. Alignment tolerance data indicate that adjustment precisions of approximately 5µm are insufficient to control the aberrations resulting from this misalignment, suggesting that adjustment precisions nearer 1µm are required for good control of misalignment aberrations. These tolerances indicate that all final alignment must be performed in-situ, using interferometric measurement of these residual aberrations as alignment references.

Table 2. A table of design alignment sensitivities for CGH1 resulting from a specific misalignment, presented as Fringe Zernike coefficients and expressed in nm wavefront.

Zernike Coefficient	Zernike Term	Piston (0.1 mm)	Rotation (0.2 deg)	X Shear (0.1 mm)	Y Shear (0.1 mm)	X Tilt (0.02 deg)	Y Tilt (0.02 deg)
2	$\rho \cos(\varphi)$	0	0	21784.4	0	0	13796.3
3	$\rho \sin(\varphi)$	5.6	0	-3.9	21841.7	-13843.8	-2.3
4	$2\rho^2 - 1$	-592.8	0	-2.7	-20.9	3.8	-2.9
5	$\rho^2 \cos(2\varphi)$	6.4	0	-2.8	41.5	-15.9	-3.1
6	$\rho^2 \sin(2\varphi)$	0	0	-38.4	0	0	-19.0
7	$(3\rho^2 - 2)\rho \cos(\varphi)$	0	0	-8.8	0	0	-256.4
8	$(3\rho^2 - 2)\rho \sin(\varphi)$	2.8	0	0	-8.4	258.9	0
9	$6\rho^4 - 6\rho^2 + 1$	1.8	0	-0.1	0	-1.0	-0.2

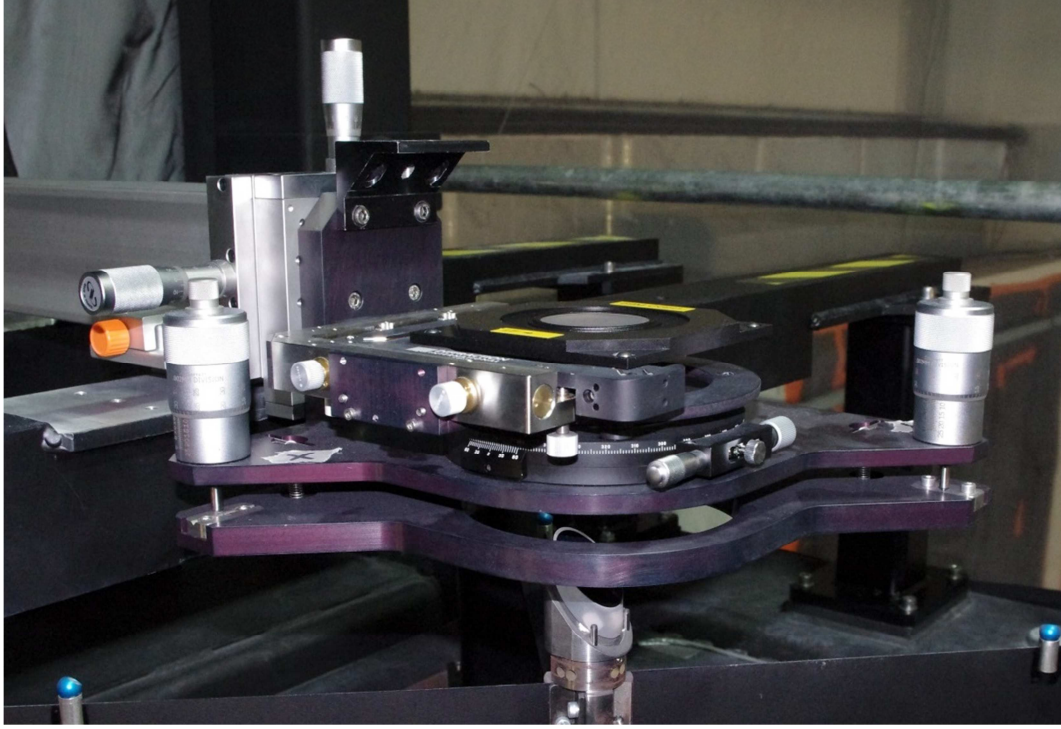Figure 5 presents a photograph of the CGH alignment assembly, integrated into the optical test.

Figure 5. A photograph of the optical test calibration assembly in use in the segment optical test. The fold mirror can clearly be seen below the calibration assembly. The diffractive imitator sits at the top of the adjustment assembly facing down.

Calibration Procedure

Consider S to represent the actual optical surface of a segment:

$$S = S(x, y) \tag{3}$$

The actual surface, S, will differ from the ideal surface, R, by an error map, E:

$$S = R + E \tag{4}$$

In optical fabrication the error map, E, is used to correct the optical surface, S, in order to converge to the reference surface, R, using some form of polishing technology.

For the testing of E-ELT prototype segments, the error map is measured using a full-aperture interferometric test with the segment supported on a bespoke testing support. The optical test is designed to produce a wavefront at the segment that will null the reflected wavefront from a perfect segment surface form. However, this test is not exact. There are a number of sources of inaccuracy in this error map resulting from the test system:

1. Test design – The test design may not be exact, there may be residual errors resulting from the test design.

2. Fabrication of test optics – There will be fabrication errors in the test optics that need to be characterized.

3. Misalignment of test optics – The test optical system will be integrated to a set of alignment tolerances designed to minimize the departure of the test wavefront from the design wavefront. Also, temperature and atmospheric variations during the testing will affect both the alignment of the test and the measured wavefront in the time domain.

4. Residual support errors – For large optics, small hysteretic support errors will vary the form of the measured surface. Whilst these support errors will be designed to be small, they will have a quantifiable effect on the test results.

Thus the measured error map, E', is related to the exact surface error, E, as follows:

$$E' = E + D + T + t \qquad (5)$$

where D is the departure of the optical test design from that defined by the reference surface; T is the departure of the actual test from the test as designed; t is the surface residual between the effect of the actual testing support and an ideal testing support. These error sources combine linearly.

In what follows, it is assumed that the nett support-induced error, t, is zero, but that it has an attributed uncertainty (attributed to support hysteresis). Thus, the actual error map is related to the measured error map by the Equation (6):

$$E = E' - D - T = E' - C \qquad (6)$$

Where,

$$C = D + T \qquad (7)$$

is the test calibration. To summarise: T represents the calibration adjustment, required to modify the as-made optical test to the test as designed; D represents an adjustment required to modify the designed test to an "ideal" test.

As noted previously, two test configurations are adopted: one configuration is required for the measurement of the reference sphere, the other configuration is required for the measurement of the ELT segment. Specifically, the reference sphere configuration is used as the ROC reference for the test, but it is also useful for quantifying other errors in the test system.

The optical arrangement of the test can be separated into several larger functional blocks. We choose:

1. Optical breadboard, including the folding flat (Figure 2)
2. Top sphere
3. Test artefact (either Reference Sphere or ELT segment)

We attribute contributions to the test calibration adjustment, T, from the following:

- optical breadboard (denoted "bb")
- top sphere (denoted "ts")
- A misalignment contribution resulting from misalignment between the top sphere and the breadboard (denoted "c")

Thus, for the reference sphere configuration, the test calibration, $C(Ref)$, may be written:

$$C(Ref) = T_{bb}(Ref) + T_{ts}(Ref) + T_c(Ref) + D(Ref) \qquad (8)$$

and similarly for the ELT segment configuration:

$$C(Seg) = T_{bb}(Seg) + T_{ts}(Seg) + T_c(Seg) + D(Seg) \qquad (9)$$

Because there are two CGH imitators that can be used to calibrate the breadboard (CGH1 for the reference sphere and CGH3 for the segment S3), it is possible to experimentally determine the breadboard error, $T_{bb}(Ref)$ and $T_{bb}(Seg)$, to a high degree of accuracy. Because the reference sphere has a surface form that is already known with high degree of accuracy, it is possible to determine $C(Ref)$. Thus for the reference sphere configuration, it is possible to quantify $T_{ts}(Ref) + T_c(Ref)$ using directly measurable surfaces.

The optical breadboard error for the segment test configuration, $T_{bb}(Seg)$, is determined from the use of the diffractive imitator, CGH3. A similar treatment is used to quantify the calibration for the ELT segment error map to give

$$C(Seg) = T_{bb}(Seg) + T_{ts}(Ref) + T_c(Ref) + D(Seg) \qquad (10)$$

In the foregoing, the two imitator CGHs are assumed to have zero error. Whilst this is a good approximation, each imitator has an attributed fabrication and alignment uncertainty.

4. RESULTS

Figure 6 presents C(Seg). The low-order aberrations are dominated by power, X-axis astigmatism, coma and X-axis trefoil. Of these, power, astigmatism and trefoil are attributed to prescription drift of the test refractive optics. Coma is attributed to misalignment. This coma is the result from misalignments in the optical test, but will include a residual from the alignment of the calibration artefacts within the test. In total, these low-order aberrations account for approximately 71 nm RMS surface error.
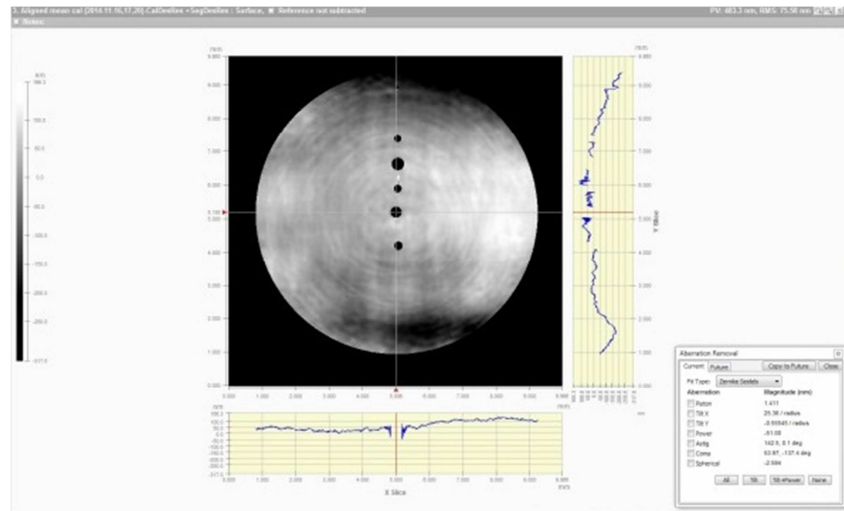

Figure 6. Surface error map of the segment test calibration. The deleted data are areas of internal reflection in the interferogram.

Removing the low-order aberrations reveals the mid-spatial errors in the test: Figure 7. Here it can be seen that the midspatial content of the calibration amounts to 24 nm RMS surface error. The linear features in this surface map are the results of linear MRF® treatments of two cylinder optics. The circular features again result from the MRF® treatment of three optical surfaces.

Table 3 presents an uncertainty analysis of these data, i.e for a single calibration test. This table indicates that the uncertainty in the calibration is dominated by the alignment of the diffractive imitators in the optical test.

An elevation in pixel-pixel noise is apparent in surface maps derived from calibration data from these diffractive imitators. This is in part attributed to low levels pixel-pixel of noise being built up by the arithmetical manipulation of surface data as described above, but may also be the result of residual speckle from the ground rear surfaces of the CGH artefacts.
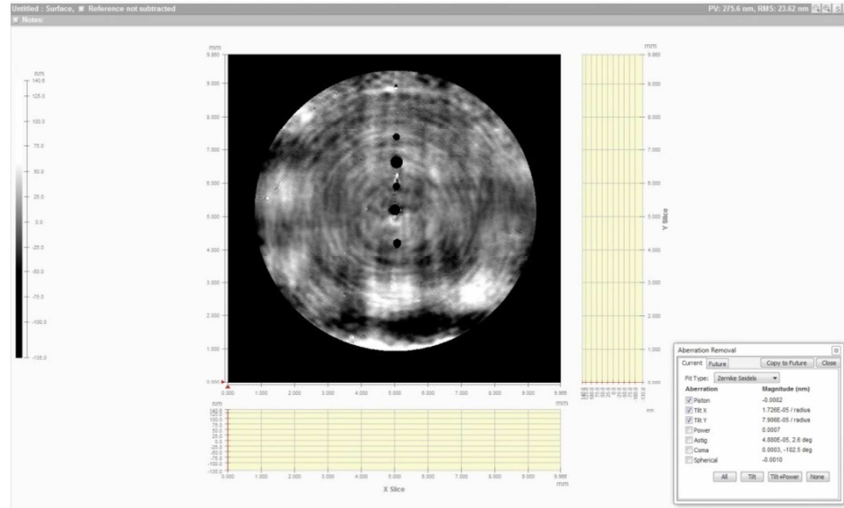
Figure 7. Surface error map of the segment test calibration, as per Figure 6, but with the low-order aberrations removed. This reveals the midspatial detail in the calibration.

Table 3. Uncertainty analysis for the use of diffractive imitators as calibration artefacts in an ELT segment test. These uncertainties represent one calibration test.

Source	Wavefront RMS (nm)
CGH1	
CGH Design Error	1
CGH Fabrication Error	3.9
CGH Measurement Repeatability	1.7
Intermediate-term Aberration Drift	0.9
CGH4	
CGH Design Error	4
CGH Fabrication Error	6.5
CGH Measurement Repeatability	2.9
Intermediate-term Aberration Drift	2.6
CGH-borne Error	**8.6**
Modelled CGH Alignment	**17.3**
Measurement Repeatability	**2.8**
Combined Uncertainty	**19.5**

5. CONCLUSIONS

In summary, we have used a set of diffractive imitator CGH artefacts to provide the traceability between two optical test configurations to high accuracy. We have demonstrated that the impact of the fabrication quality of the diffractive imitators used in our application is significantly less than the impact of the alignment of the imitator within the test.

In use, the gain in knowledge of the residual aberrations of a multi-element system resulting from the use of diffractive artefacts can be significant and can substantially improve fabrication quality. We note that the duration of the calibration

process was dominated by the alignment of the diffractive imitators. It is clear that alignment also dominates the remaining uncertainties of this approach to calibration. Whilst this approach is not a substitute for the manufacture of high quality test optics, it is a highly effective way of understanding the performance of existing optical systems.

Whilst absolute error is attributed to the CGH-based calibration, there is more work to be done on traceability of CGH-borne errors to the International standard of length.

REFERENCES

[1] Grey, C., Baker, I., Davies, G., Evans, R., Field, N., Fox-Leonard, T., Messelink, W., Mitchell, J., Rees, P., Waine, S., Walker, D.D., Yu, G., "Fast manufacturing of E-ELT mirror segments using CNC polishing" Proc. SPIE 8838, 88380K-88380K-12 (2013).
[2] A.G. Poleshchuk, E.G. Churin, V.P. Koronkevich, V.P. Korolkov. "Polar coordinate laser pattern generator for fabrication of diffractive optical elements with arbitrary structure," Appl. Opt., **38**, 1295-1301 (1999).
[3] V.P. Veiko, V.I. Korolkov, A.G. Poleshchuk, A.R. Sametov, E.A. Shakhno, M.V. Yarchuk. "Study of the spatial resolution of laser thermochemical technology for recording diffraction microstructures," Quantum Electronics, **41**, 7, 631-636 (2011).